Int. J. Electrochem. Sci., 12 **(2017)** 5104 – 5120, doi: 10.20964/2017.06.13

International Journal of
ELECTROCHEMICAL
SCIENCE
www.electrochemsci.org

Corrosion Behaviour of T92 Steel in NaCl Solution

Yi Long[1,2], *Chao Feng*[1,2], *Bicao Peng*[1,2], *Yi Xie*[1, 2], *Jun Wang*[1,2], *Minghua Zhang*[3], *Yuanhui Wu*[4], *Tangqing Wu*[3,*], *Fucheng Yin*[3]

[1] Electric Power Research Institute, State Grid Hunan Electric Power Company, Changsha 410007, China;
[2] Hunan Xiangdian Boiler & Pressure Vessel Inspection Center co., LTD, Changsha 410001, China;
[3] Key Laboratory of Materials Design and Preparation Technology of Hunan Province, Xiangtan University, Xiangtan 411105, China
[4] School of Chemistry and Chemical Engineering, Zunyi Normal College, Zunyi 563002, China
[*]E-mail: tqwu10s@alum.imr.ac.cn

Received: 23 January 2017 / *Accepted:* 18 March 2017 / *Published:* 12 May 2017

In the paper, the effects of NaCl on the corrosion behaviour of T92 steel at room temperature were studied by neutral salt spray test, electrochemical technology and scanning electron microscope. The results show that the corrosion rate of T92 steel continuously increase with the NaCl concentration during the neutral salt spray tests. NaCl promotes the anodic process rather than the cathodic process of the T92 steel in solution. In NaCl solutions with low concentrations, T92 steel undergoes uniform corrosion, wheres its corrosion behaviour will develop into pitting as the concentration of NaCl increase. The formation and development mechanism for the corrosion pitting are also discussed in the paper.

Keywords: T92, salt spray test, electrochemical impedance spectroscopy (EIS), scanning electron microscope (SEM), pitting

1. INTRODUCTION

In compliance with the power industry requirements for energy efficiency, low-consumption and environment protection, power-generation equipment is moving towards larger-capacity tendencies, as the steam conditions being used are also moving towards higher temperatures and pressures. As is known, supercritical and ultra-supercritical generating units, which are highly efficient, are being developed by many Euro-American developed countries. Subcritical and supercritical generating units have been used in the power industry in China, and good environmental

results and considerable economic profits have been achieved. For safety, high anti-oxidation, high creep-resistant and superior processability properties are necessary for pipes used in subcritical, supercritical and ultra-supercritical generating units to operate in the rigorous steam conditions. T92 pipe, developed by researchers in the United States, can meet almost all these needs, and has been selected as the main heat-resistant material and renewal material for the main steam piping in supercritical generating units [1]. For safety, it is vital to study the corrosion behaviour of this steel during storage and service to identify the key aspects that affect its service life and structural safety.

To date, systematic studies have been conducted on the oxidation behaviour of the T91 alloy at temperatures of 500~700 °C [2-4]. Many studies show that the material obeys the parabolic law for the growth of corrosion products on the surface of Ferritic/Martensitic steel in supercritical water and steam [5, 6]. Additionally, the oxide features a bi-layer structure, including Fe oxide and other alloying elements in the inner layer and Fe_3O_4 and Fe_2O_3 in the external layer [6]. The corrosion products in the inner layer are dense and integrated, which provide a protection to the matrix, whereas the corrosion products in the external layer are loose and porous, tending to experience flake peeling from the alloy surface [7].

Further studies have found that the interface between the inner and external layers of the corrosion products is the original alloy surface [8]. The result indicates that corrosion products in the inner layer are generated by the internal diffusion of oxygen, whereas those in the external layer are produced by the external diffusion of positive ions [9]. Zhang et al. experimentally observed the internal and external oxidation behaviours of T91 steels [10]. Li et al. determined that a combined treatments of shot blasting and deposited RE (rare earth) coating can decrease the parabolic rate constant and effectively improve the anti-oxidation properties of the T91 alloy. From this discussion, we conclude that in-depth and systematic studies have been performed on the corrosion behaviour of the T91 alloy in service conditions, and effective protection methods have been proposed.

In engineering practice, prior to service, the T91 alloy usually needs to be placed in certain natural environment, where it is exposed to erosion in the atmosphere. This phenomenon has been observed in engineering practice, and few studies have been conducted in laboratory. Zhang et al. reported that T91 seamless steel pipes with shot blasting have experienced partial corrosion on the inner and outer surfaces after a one-year storage period in Zigong City, Sichuan Province, China [11]. Based on the characteristics of the natural environment and the properties of T91 steels, the authors concluded that the seasonal acid rain and the atmospheric environment in the heavy-industry zone are the major causes of the partial corrosion of T91 steel during storage. From this work, reasonable suggestions were proposed [12]. Yu et al. studied the influence of pH and Cl^- as part of the electrochemical corrosion behaviour of T92 steel at room temperature and found that Cl^- can corrode the passive film of T92 steels [13]. This result is valuable for predicting the corrosion behaviour of T92 steel in natural environment storage.

Our company has also determined the partial corrosion behaviour of T91 steels during storage in natural environments. However, as discussed, there is a lack of work on this topic. In the paper, the effect of NaCl on the corrosion behaviour of T92 steel at room temperature is studied using neutral salt spray testing, electrochemical technology and scanning electron microscope.

2. MATERIAL AND METHODS

2.1 Materials

The material used in this work is T92 pipe steel. The chemical composition of this material (wt. %) is shown in Table 1. Specimens were machined to dimensions of 10 mm × 10 mm × 3 mm and embedded in epoxy resin, leaving an area of 10 mm × 10 mm exposed for electrochemical measurements. Other specimens were machined to dimensions of 30 mm × 20 mm × 3 mm for neutral salt spray testing. The working surface of the specimens was abraded mechanically with a series of grit papers (400#, 600#, 800#, and 1000#) according to the national standards GB5776-86 and then cleaned successively in acetone and alcohol.

Table 1. Chemical compositions of T92 steel

Element	Content (wt.%)
C	0.12
Si	0.18
Mn	0.5
Cr	8.96
Nb	0.068
Mo	0.36
Ni	0.13
P	0.013
S	0.005
Al	0.01
N	0.062
W	1.75
V	0.18
Fe	Bal.

2.2 Neutral salt spray test

Salt spray test is a useful method for corrosion resistance evaluation of materials used in atmospheric environment [14, 15]. The neutral salt spray test samples were hung in a salt-spray chamber using a nylon thread and exposed to different concentration (0.5%, 1.0%, 5.0% and 10%) NaCl solutions. The test environment was conducted accord to the ASTM B117 standard specifications. The temperature was 35±2°C inside the salt-spray chamber. The neutral salt spray test times were 25, 50, 75, and 100 h, respectively. After the neutral salt spray test treatment, the corrosion products on the steel surface were removed using a rust removing solution composed of water (500 mL), hydrochloric acid (500 mL), and hexamethylenetetramine (20 g). Afterwards, the mass loss was calculated.

2.3 Electrochemical measurements

The electrochemical properties of the steel in the NaCl solutions were investigated via electrochemical impedance spectroscopy (EIS) and Tafel polarization curves. A three-electrode electrochemical cell was used to perform all the electrochemical experiments, with a saturated calomel electrode (SCE) as the reference electrode and a platinum electrode as the counter electrode. The test was operated using a CS350 electrochemical measurement system manufactured by Wuhan CorrTest Instruments Corp., Ltd. The frequency range for the EIS was from 100 kHz to 10 mHz, and the amplitude of the sinusoidal voltage signal was 10 mV. The potential scanning velocity for the Tafel polarization was 0.25 mV s^{-1}, and the overall scope was ± 250 mV. The results were modelled and simulated using the Origin software package.

2.4 Analysis of Corrosion Products

After the electrochemical experiment was performed for 15 days, the exposed surface of the T92 steel was cleaned in 100% alcohol for ten minutes, dried in a cold air flow, and stored in an oxygen-free desiccator for corrosion product analysis. The morphologies of both the corrosion products and the corroded surface were obtained using a scanning electron microscope (JSM-6360LV). Prior to the corrosion attack surface examination, the steel surface corrosion products were removed using the same rust removing solution described above.

3. RESULTS AND DISCUSSION

3.1 Weight loss

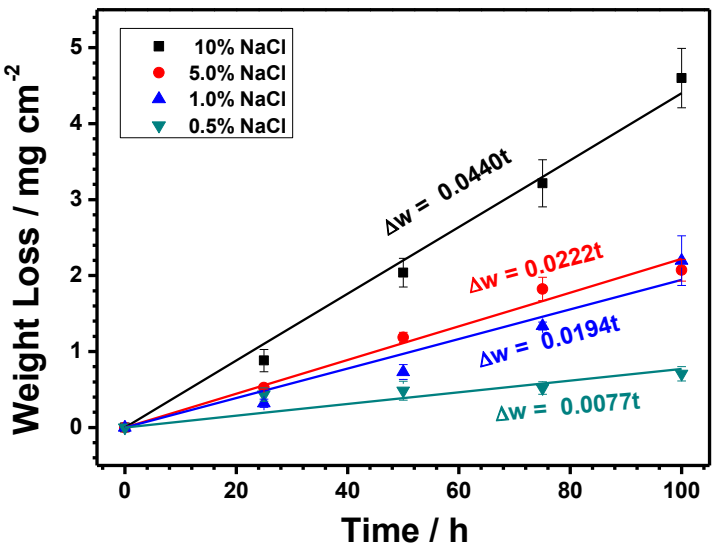

Figure 1. Mass loss from the T92 steel as a function of exposure time in the different NaCl solutions

The mass loss curves for the T92 steel in the salt spray tests for different NaCl concentrations are shown in Fig. 1. In general, the corrosion mass loss for the T92 steel linearly increased with the NaCl solution concentration (the error in the 0.5% NaCl solution is greater than those in the other environments), and the corresponding fitting results are also listed in Fig. 1. In the 0.5% NaCl solution, the corrosion mass loss of the T92 steel at the earlier experimental stage is fast and increases only slightly after an experiment time of greater than 25 h. When the NaCl concentration increases to 1.0% and 5.0%, the mass loss curve for the T92 steel gradually increases with the corrosion time. From the linear fitting shown in Fig. 1, the rate constants for the T92 steel in the 1.0% and 5.0% NaCl solutions are 0.0194 and 0.0222 g cm^{-2} h^{-1}, respectively, which is approximately twice that in the 0.5% NaCl solution. In the 10% NaCl solution, the corrosion mass loss also increases with time, with the rate constant being 0.044 g cm^{-2} h^{-1}, which is the fastest corrosion rate obtained during the experiments. The results show that the corrosion rate of the T92 steel continuously increases with the NaCl concentration [16].

3.2 EIS Analysis

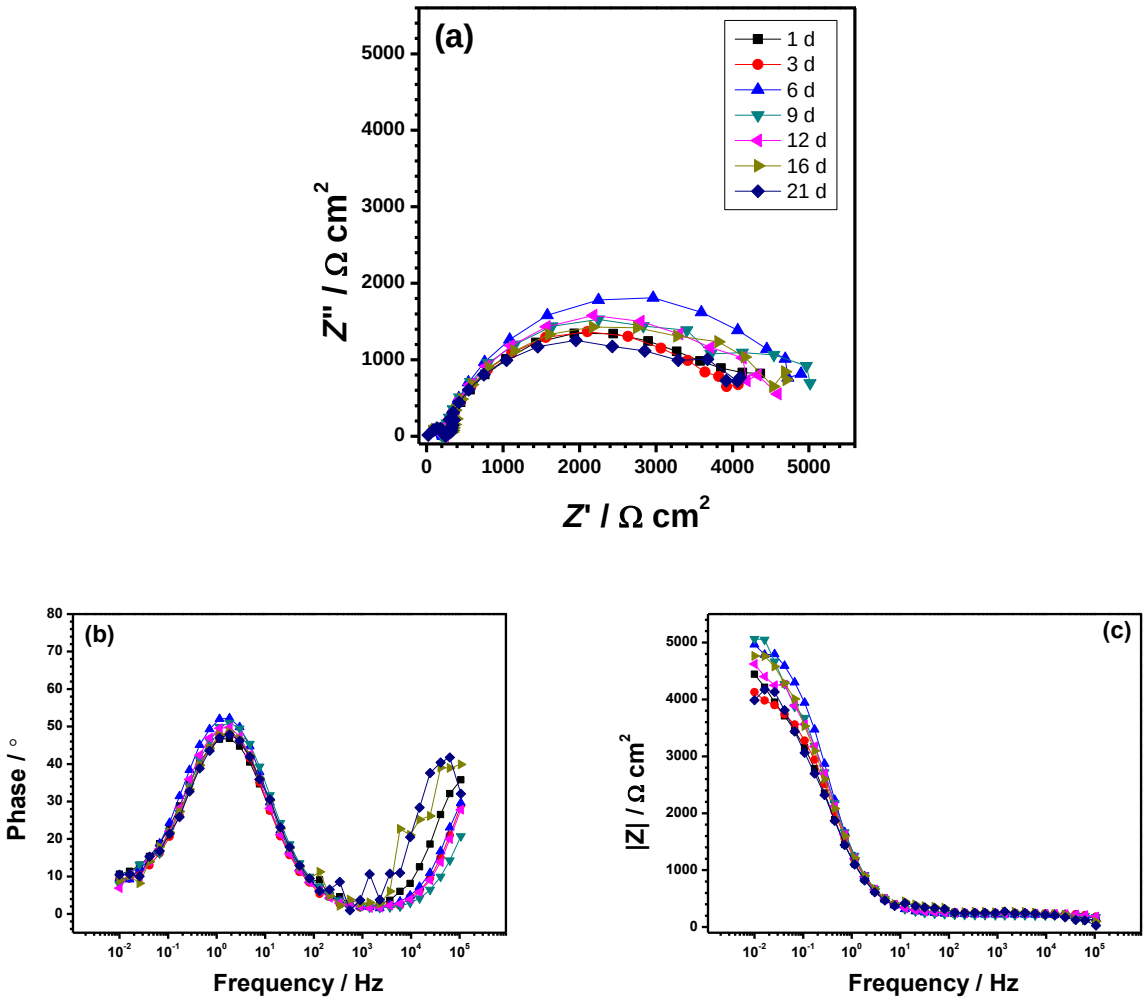

Figure 2. Evolution of EIS of the T92 steel in 0.1% NaCl solution as a function of time

The EIS evolution of the T92 steel in the 0.1% NaCl solution is shown in Fig. 2. On the first and third days of the experiment, the EIS plots show two capacitance arcs and one Weber impedance, and the corresponding fitting result is listed in Table 2. Afterwards, the Weber impedance disappears, and the EIS plots for the T92 sample manifest two capacitance arcs. The capacitance arc in the high frequency section concerns the high frequency phase shift and high solution resistance, whereas the capacitance arc in the low frequency section is related to the electric double layer on the sample surface. The solution resistance is between 40 and 50 Ω cm^2 and does not change significantly during the entire experiment. Since the concentration of the NaCl is low (0.5%), the conductivity of the solution is relatively low, resulting in a relatively high solution resistance. During the entire experimental process, the charge transfer resistance of the T92 steel tends to decreases as the experiment time is lengthened, indicating that the corrosion rate of the steel gradually accelerates.

Table 2. Fitting results from the EIS data for the T92 steel in the 0.1% NaCl solution as a function of time

Time (h)	R_s ($\Omega\cdot cm^2$)	Y_f ($S\cdot sec^n\cdot cm^{-2}$)	n_f	R_f ($\Omega\cdot cm^2$)	Y_{dl} ($S\cdot sec^n\cdot cm^{-2}$)	n_{dl}	R_{ct} ($\Omega\cdot cm^2$)	Y_W ($S\cdot sec^5\cdot cm^{-2}$)	χ^2
2	52.66	3.104×10^{-8}	0.9514	176.1	1.964×10^{-4}	0.7832	3733	5.235×10^{-3}	2.97×10^{-4}
72	53.7	1.252×10^{-8}	0.9579	185.7	1.696×10^{-4}	0.8145	3598	6.746×10^{-3}	2.19×10^{-4}
144	45.2	2.298×10^{-8}	0.9247	175.7	1.673×10^{-4}	0.8135	4899	-	6.52×10^{-4}
216	45.22	1.124×10^{-8}	0.9419	161.6	1.729×10^{-4}	0.7856	4757	-	1.66×10^{-3}
264	25.29	1.449×10^{-8}	0.9204	209.2	1.747×10^{-4}	0.8028	4395	-	5.65×10^{-4}
384	38.60	1.400×10^{-7}	0.8564	238.9	1.907×10^{-4}	0.7471	4710	-	1.19×10^{-2}
504	43.41	5.799×10^{-8}	0.9457	237.6	1.974×10^{-4}	0.7317	4564	-	2.52×10^{-2}

Table 3. Fitting results from the EIS data for the T92 steel in the 1.0% NaCl solution as a function of time

Time (h)	R_s ($\Omega\cdot cm^2$)	Y_f ($S\cdot sec^n\cdot cm^{-2}$)	n_f	R_f ($\Omega\cdot cm^2$)	Y_{dl} ($S\cdot sec^n\cdot cm^{-2}$)	n_{dl}	R_{ct} ($\Omega\cdot cm^2$)	χ^2
2	24.04	3.718×10^{-6}	1.000	1.598	3.408×10^{-4}	0.7788	2492	8.87×10^{-3}
72	27.62	6.747×10^{-4}	0.7054	180.5	8.805×10^{-5}	0.9734	1990	5.47×10^{-3}
144	29.70	5.991×10^{-4}	0.7171	90.42	2.243×10^{-4}	0.8616	2942	6.53×10^{-3}
216	27.66	7.911×10^{-4}	0.6905	160.3	1.103×10^{-4}	0.9383	1951	5.21×10^{-3}
264	24.66	6.759×10^{-4}	0.7291	93.81	3.000×10^{-4}	0.8296	2335	5.86×10^{-3}
384	24.60	7.955×10^{-4}	0.6829	120.8	2.516×10^{-4}	0.8062	1697	8.20×10^{-3}
504	24.98	7.051×10^{-4}	0.7075	92.70	3.935×10^{-4}	0.7609	1775	8.87×10^{-4}

The EIS evolution of the T92 steel in the 1.0% NaCl solution is shown in Fig. 3 and features a depressed capacitance arc in the Nyquist plot (Fig. 3a). In the Bode plot (Fig. 3b), two time constants are obtained in the low frequency section, where one reflects an electric double layer feature and the other is related to the corrosion products on the steel surface [17]. Therefore, the depressed capacitance arc in Fig. 3a is superposed by two capacitance arcs. The corresponding fitting results are shown in Table 3. The solution resistance is between 20 and 30 Ω cm2, which is smaller than that in the 0.1% NaCl solution. During the entire experiment, the charge transfer resistance of the T92 steel tends to

decrease as the experiment time increases, which implies that the corrosion rate of the steel gradually accelerates. Compared to the 0.1% NaCl solution, the charge transfer resistance of the steel decreases, which indicates that the Cl^- ions promote the corrosion process in the T92 steel [16].

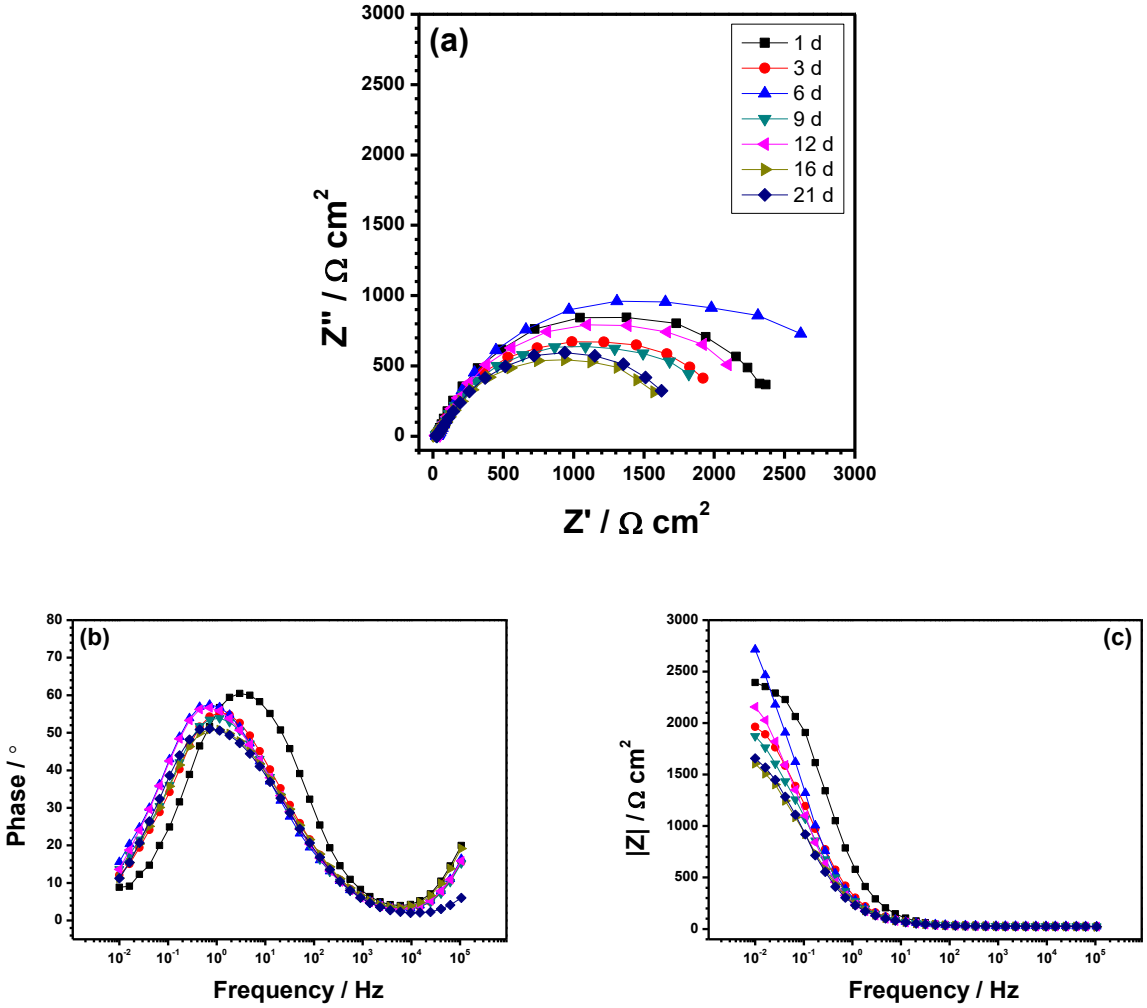

Figure 3. Evolution of EIS of the T92 steel in1.0 % NaCl solution as a function of time

The EIS evolution of the T92 steel in the 10% NaCl solution is shown in Fig. 4. Although the solution concentration further increases, the EIS plots still exhibit a single depressed capacitance arc (Fig. 4a), which is similar to the previous phenomenon. The fitting results are shown in Table 4. Due to the high concentration of the NaCl, there is excellent solution conductivity, and the solution resistances are distributed between 3 and 4 Ω cm^2 in the 10% NaCl solution. On the first day of the experiment, the charge transfer resistance for the T92 steel is very high (≈ 4556 Ω cm^2), and the corrosion rate is low. This may be caused by the Cl^- with a high concentration adsorbing on the metal surface, which may impede the arrival of oxygen. During the entire experimental process, the charge transfer resistance of the T92 steel decreases with time, showing that the corrosion rate of the steel gradually accelerates.

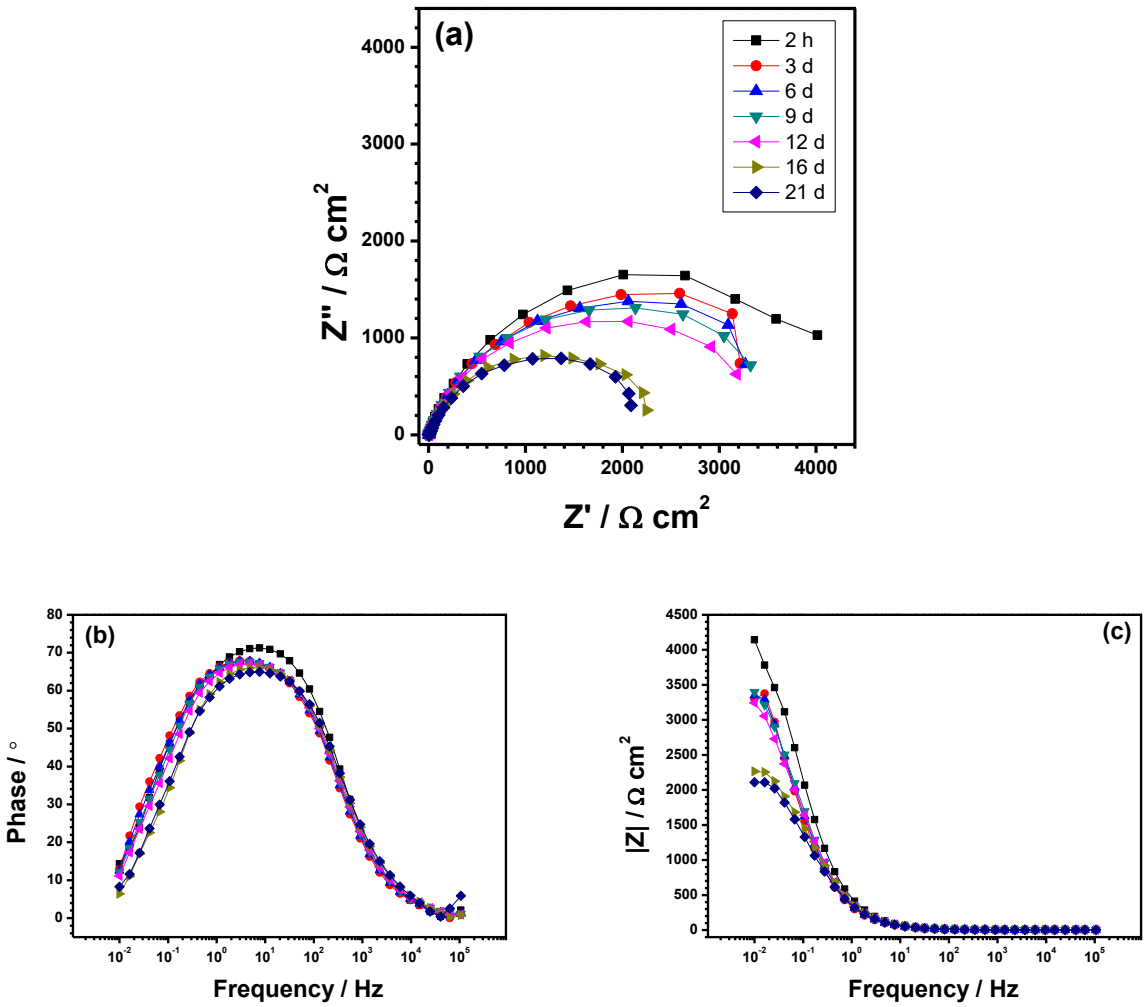

Figure 4. Evolution of EIS of the T92 steel in 10 % NaCl solution as a function of time

Table 4. Fitting results from the EIS data for the T92 steel in the 10% NaCl solution as a function of time

Time (h)	R_s ($\Omega \cdot cm^2$)	Y_f ($S \cdot sec^n \cdot cm^{-2}$)	n_f	R_f ($\Omega \cdot cm^2$)	Y_{dl} ($S \cdot sec^n \cdot cm^{-2}$)	n_{dl}	R_{ct} ($\Omega \cdot cm^2$)	χ^2
2	3.272	6.294×10^{-5}	0.9926	1.596	4.374×10^{-4}	0.7651	4556	3.74×10^{-4}
72	3.430	3.630×10^{-4}	0.8194	2.929	3.381×10^{-4}	0.7465	4011	4.53×10^{-4}
144	3.480	2.552×10^{-4}	0.8389	2.197	4.007×10^{-4}	0.7464	3896	2.4×10^{-4}
216	3.514	4.812×10^{-4}	0.7741	4.500	1.296×10^{-4}	0.8292	3758	1.83×10^{-4}
264	3.557	5.260×10^{-4}	0.7647	6.329	8.240×10^{-5}	0.8630	3497	2.69×10^{-4}
384	3.513	2.137×10^{-4}	0.8377	2.580	3.673×10^{-4}	0.7450	2421	2.31×10^{-4}
504	3.221	5.880×10^{-4}	0.7545	7.698	6.196×10^{-5}	0.8642	2331	4.69×10^{-4}

Compared to the 0.1% and 1.0% NaCl solutions, the charge transfer resistance of the steel is highest (indicating the lowest corrosion rate) in the 10% NaCl solution, which is contradictory to the

high corrosion mass loss from the salt spray test for the same solution. This contradiction may be explained by the evolution of oxygen. In the salt spray test, the corrosion environment is the NaCl fog with gaseous or aerosol states on the steel surface. Thus, it is easy for oxygen to gain access to the steel surface (which is closer to actual conditions). However, during the immersion test, the corrosion environment is the NaCl solution, and the concentration and diffusion rate of oxygen will decrease accordingly. Therefore, the absorption intensity of the Cl^- is much greater than that of the oxygen, leading to the increasing charge transfer resistance in the 10% NaCl solution.

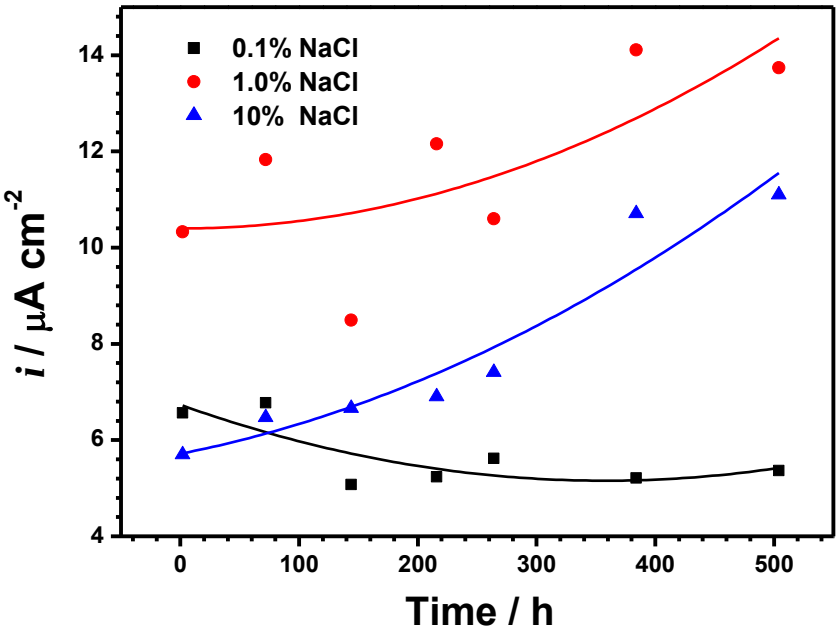

Figure 5. Corrosion current density derived from the EIS of the T92 steel in the different concentration NaCl solutions as a function of time

The corrosion current densities of the steel in different NaCl solutions were calculated from the EIS fitting results, assuming a Stern-Greary constant of 26 mV. The corrosion current densities and the corresponding variation tendencies are shown in Fig. 5 via the dashed and solid lines, respectively. The corrosion current densities in the 0.1% NaCl solution are limited and decrease throughout the experiment, indicating a decrease in the corrosion rate. However, in the 1.0% and 10% NaCl solutions, the corrosion current densities increase with time, and the corrosion current densities in the 1.0% solution are higher than those in the 10% NaCl solution. These results are consistent with the above discussion.

To further study the influence that the NaCl has on the corrosion behaviour of the T92 steel, the EIS is plotted versus the NaCl concentrations, as shown in Fig. 6. Initially, as the NaCl concentration increases, the charge transfer resistance of the T92 steel decreases, before beginning to increase [16].

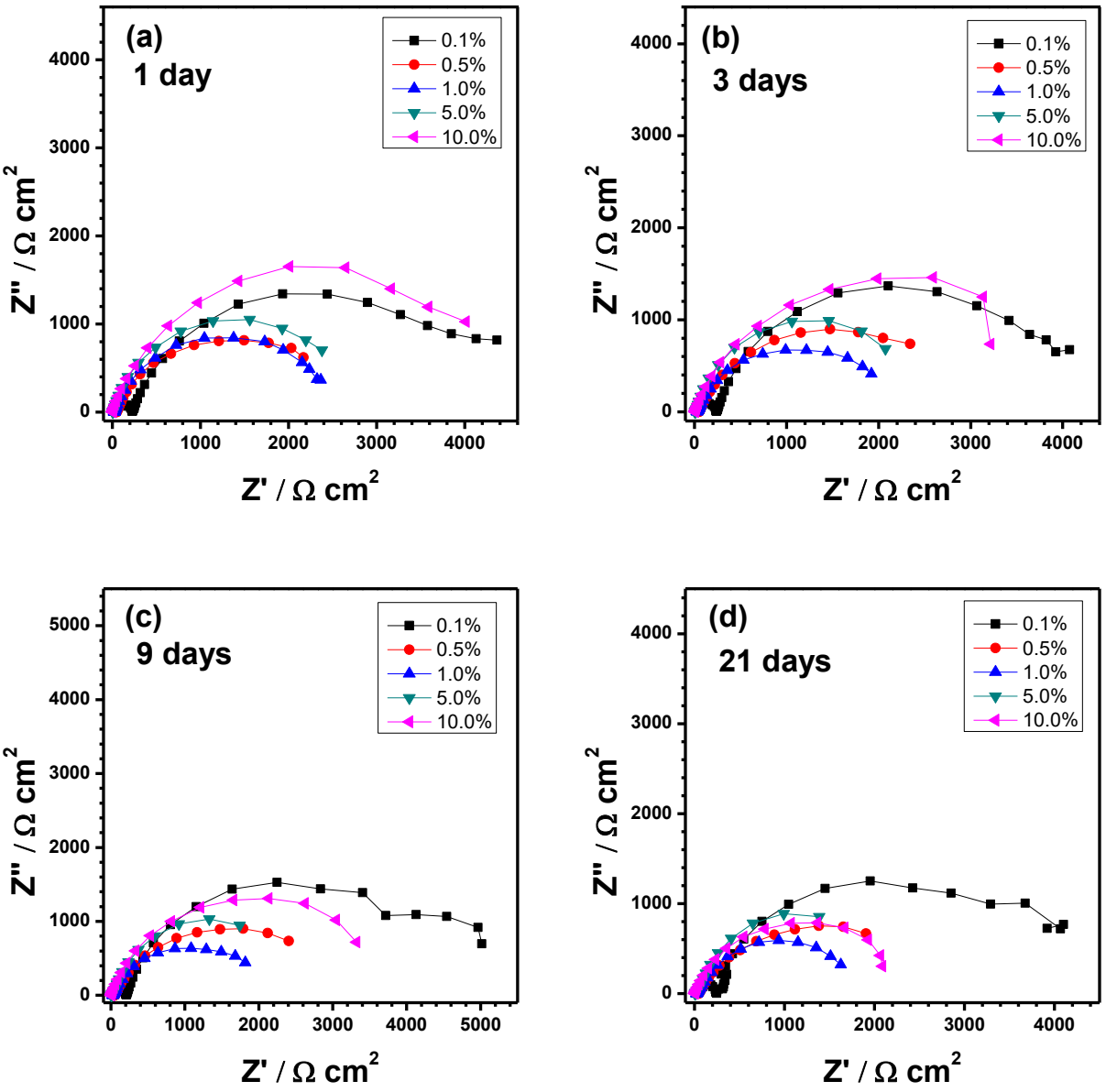

Figure 6. Evolution of the EIS of the T92 steel in the different concentration NaCl solutions

When the NaCl concentration reaches 10%, the resistance is roughly equivalent to that in the 0.1% NaCl solution. After three days of the experiment, the increasing NaCl accelerates the corrosion rate of the steel, especially the 1.0% NaCl solution. After that, the acceleration still exists and gradually intensifies.

From the above discussions, as the NaCl concentration increases, the ion concentration increases and the solution resistance decreases, enhancing the corrosion process of the T92 steel. As the concentration of NaCl increases, the corrosion rate of the T92 steel increases, reaches a maximum value in the 1.0% NaCl solution, and decreases in the high NaCl concentration (10%).

3.3 Tafel Curve

The Tafel polarization curves for the T92 steel in the different concentration NaCl solutions after 21 days are shown in Fig. 7, with the corresponding fitting results in Table 5. The increasing NaCl concentration has little effect on the cathodic polarization behaviour of the steel (which is about hydrogen evolution [18]) but has a significant influence on the corrosion potential and anodic polarization behaviour. As the NaCl concentration increases, the corrosion potential E_{corr} of the steel gradually decreases and the corrosion current density i_{corr} gradually increases, illustrating that the NaCl has accelerated the corrosion process [16]. In the different concentration NaCl solutions, the cathodic Tafel slopes (β_c) of the steel are between -400 and -520 mV/dec, whereas the anodic Tafel slope (β_a) decreases from 412 mV/dec to 133 mV/dec as the NaCl concentration increases from 0.1% to 10%. This indicates that NaCl promotes the anodic process of the T92 steels in solution.

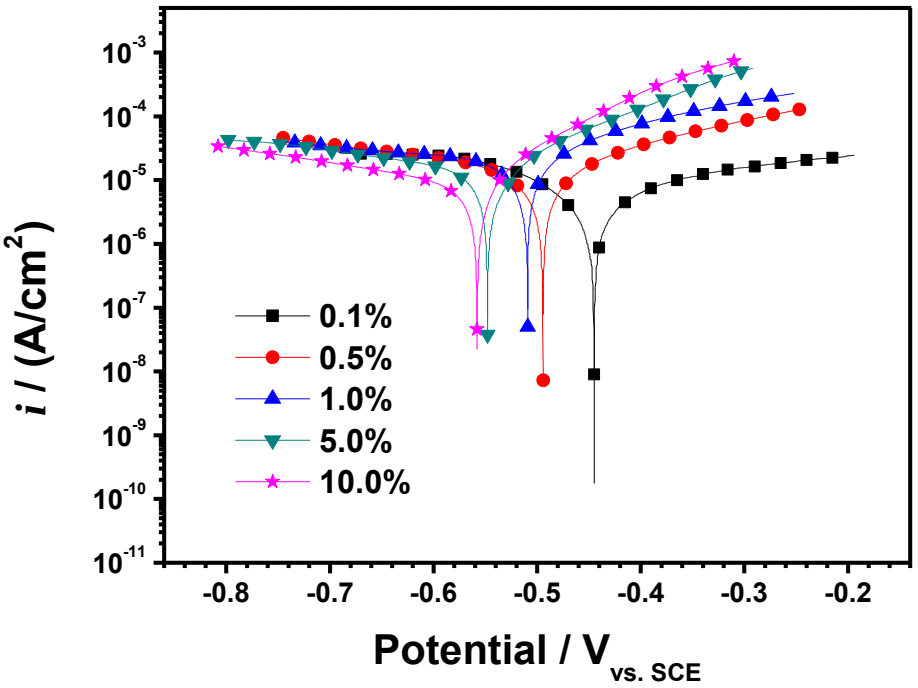

Figure 7. Tafel polarization curves for the T92 steel after a 21 day exposure to different concentrations of NaCl

Table 5. Fitting results from the Tafel polarization curves for the T92 steel after immersion for 21 days in different concentrations of NaCl

[NaCl]	E_{corr} / ($V_{vs. SCE}$)	i_{corr} / (μA cm^{-2})	β_c / (mV/dec)	β_a / (mV/dec)
0.1 %	-0.446	6.52	-404.78	412.20
0.5 %	-0.495	11.5	-489.59	367.88
1.0 %	-0.509	12.8	-513.56	212.31
5.0 %	-0.550	14.5	-459.96	181.93
10 %	-0.559	16.5	-439.62	133.72

3.4 Morphology of corrosion product

The morphologies of the corrosion products on the steel surface after a 21 day exposure in the 0.1% NaCl solution are shown in Fig. 8, with the corresponding EDS analysis results in Table 6. The machine grinding scratches on the steel surfaces are very clear, and the steel surfaces are hardly covered with any corrosion products. The EDS analysis shows that the major components on the surface are Fe and Cr.

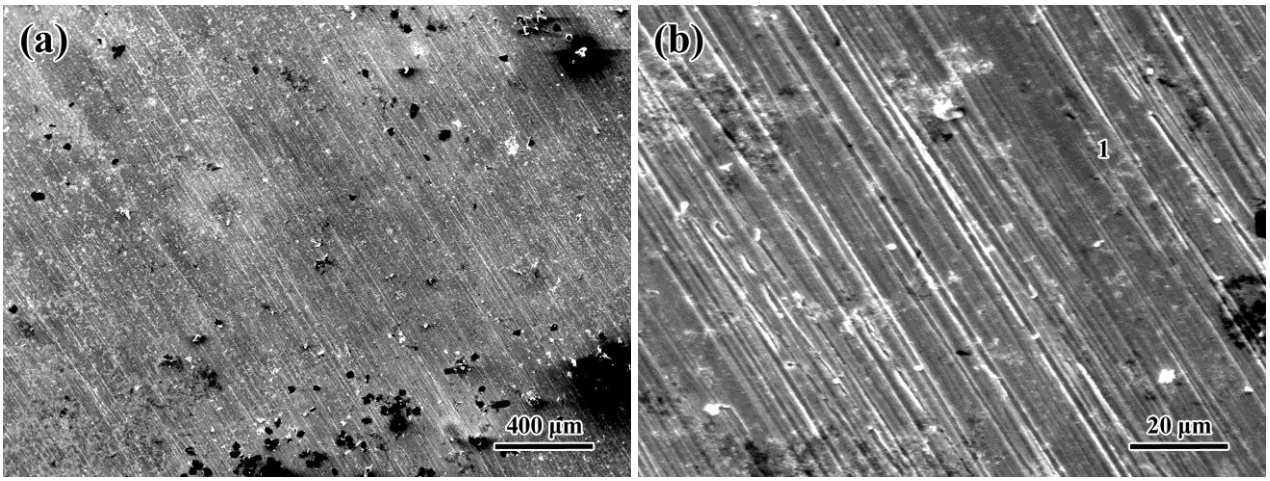

Figure 8. Corrosion surface morphologies for the T92 steel after a 21 day exposure in the 0.1% NaCl solution

Table 6. EDS results for the corrosion products shown in Figs. 7 and 8.

Position	C	O	Fe	Cr	Si	Na	Cl	W
1	-	-	91.17	8.83	-	-		-
2	26.40	30.05	11.82	25.52	-	-	1.83	2.14
3	14.18	63.87	14.56	4.46	2.08	-	0.85	-
4	19.38	-	15.26	2.20	-	36.56	26.59	-

The morphologies of the corrosion product on the steel surface after a 21 day exposure in the 1.0% NaCl solution are shown in Fig. 9, with the corresponding EDS analysis results in Table 6. After a 21 day exposure, the majority of the corrosion products on the steel surface are smooth, bright and clean. Some of the corrosion products appear block shaped and appear inclined to initiate on the edge of the steel surfaces. Their typical morphologies are shown in Fig. 8. The diameter of the block-like corrosion products is approximately 3~4 mm, with a 1~2 mm dense “core” in the central area. The “core” extends into the inside of the steel matrix, and loose corrosion products are distributed around it. The EDS analysis shows that Cr and Fe oxides are the main components of the “core” (Position 2), and the Cr content is higher than that of the Fe, which is dissimilar from the main components of the T92 steel matrix (Table 1). The corrosion products covering the “core” are also corrosion products of

Fe and Cr (Position 3) [14]. However, the Fe content here is higher than that of Cr. The main components of corrosion products around the "core" are Fe and Cr corrosion products, as well as NaCl (Position 4). In the 10% NaCl solution, similar results are obtained and are not listed in the paper.

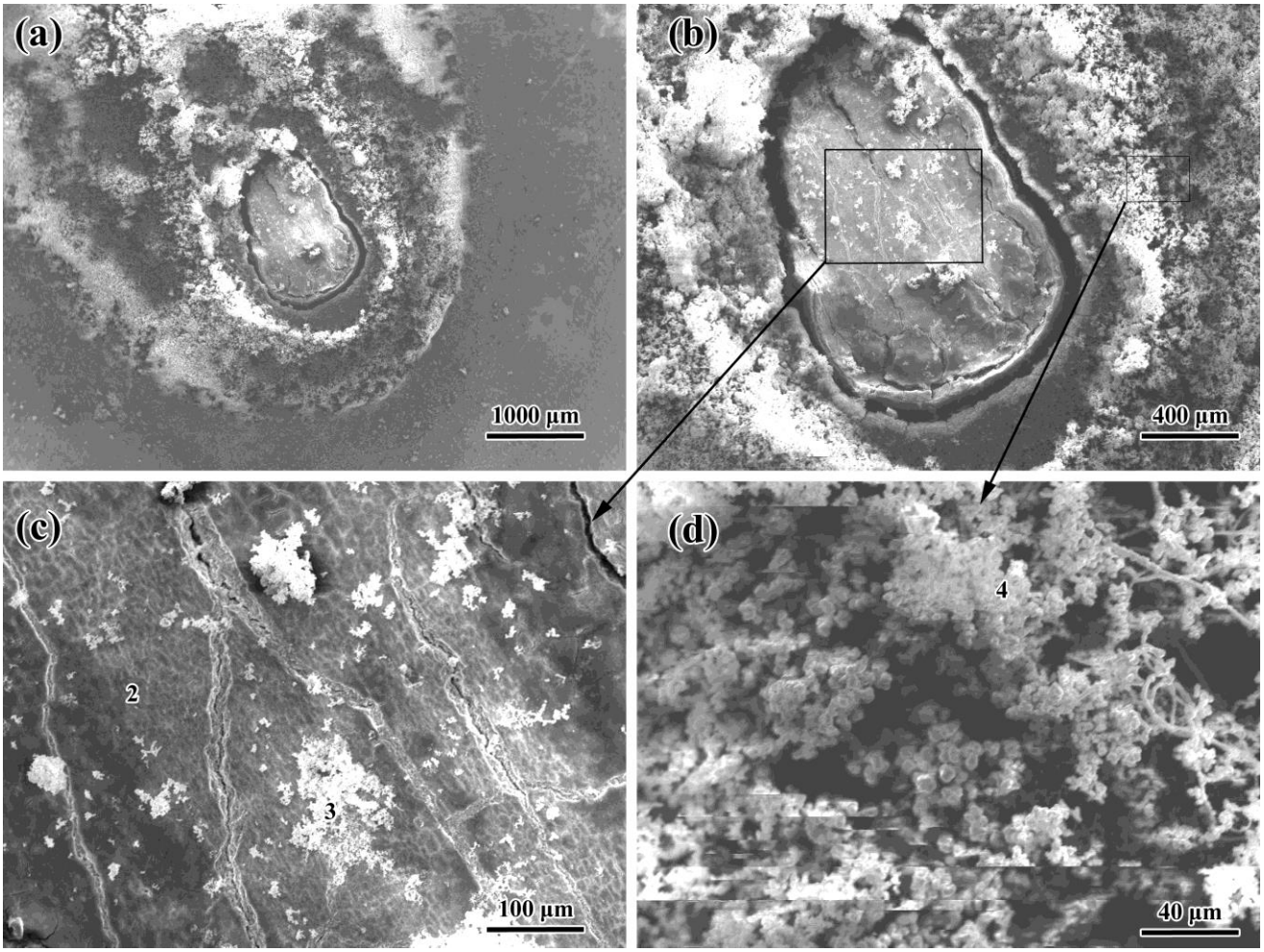

Figure 9. Corrosion surface morphologies on the T92 steel after a 21 day exposure in the 1.0% NaCl solution

Based on these results, we can reasonably speculate the generation process for the corrosion product in NaCl solution. As the NaCl concentration increases, the tendency to partially corrode the steel surface increases [15]. The corrosion products during partial corrosion contain Fe and Cr oxides, and the latter tends to form dense core-shaped corrosion products and entrains Fe oxides within it. However, Fe oxides are relatively loose and tend to attach to the "core". Cr oxides have a stable structure and high corrosion potential, meaning that they usually act as the cathode in corrosion reactions. Combined with the anodic reaction of the nearby metal matrix, the cathodic reaction occurring on the "core" will accelerate the corrosion process of the steel.

3.5 Corrosion attack morphology

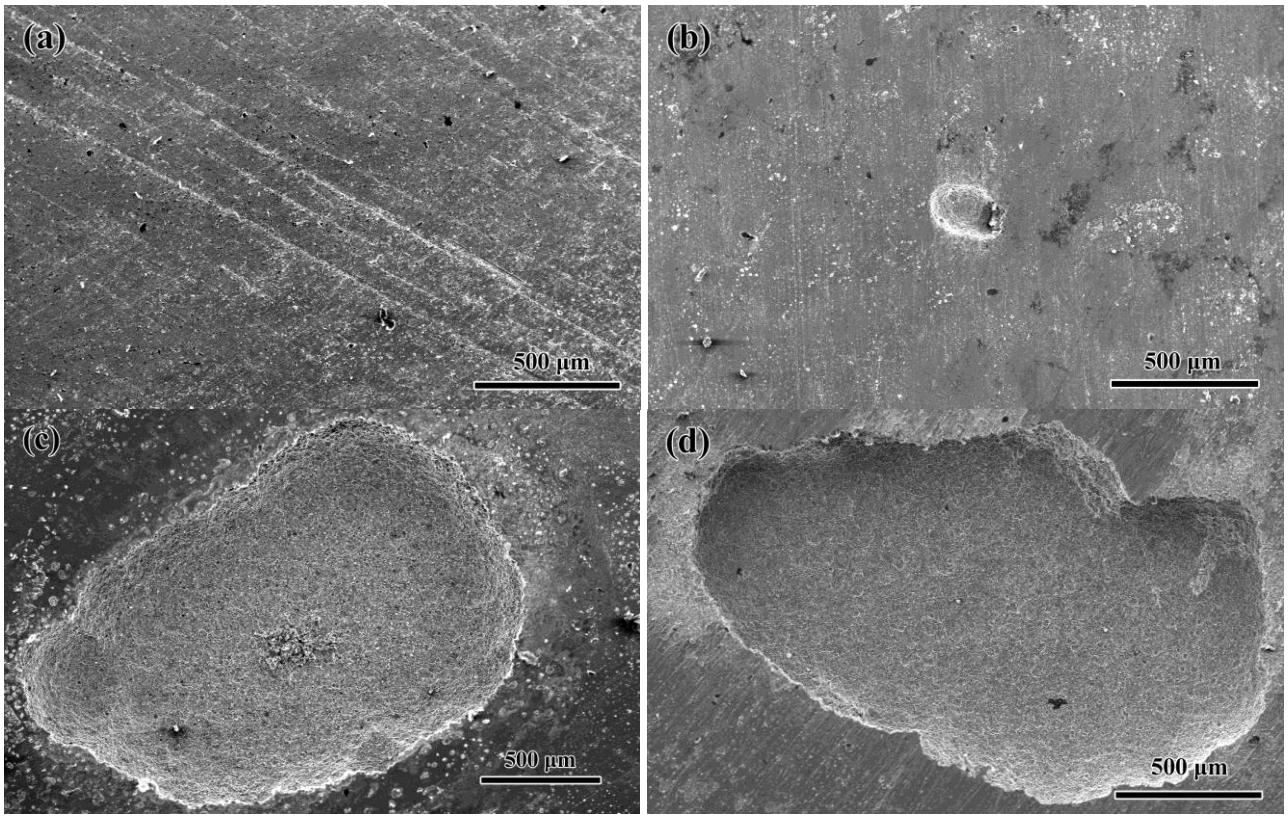

Figure 10. Corrosion attack surface morphologies for the T92 steel after a 21 day exposure in NaCl solutions with different concentrations: (a) 0.1%, (b) 0.5%, (c) 1.0%, and (d) 10%

Corrosion attack surface morphologies for the T92 steel after a 21 day exposure in NaCl solution with different concentrations are shown in Fig. 10. After a 21 day exposure in the 0.1% NaCl solution, the machine grinding scratches on the steel surface are clear and bright, without any corrosion pitting or partial corrosion features observed. It seems that corrosion only occurs on the bulges of the scratches. In the 0.5% NaCl solution, the steel surface mainly experiences uniform corrosion, with a few corrosion pits of small diameter forming. This shows that NaCl promotes the emergence of corrosion pitting. In the 1.0% NaCl solution, there are 2-3 corrosion pits with diameters of 1-2 mm generated on the steel surface, indicating that increasing the NaCl concentration improves the spreading rate of the corrosion pitting and enhances the sensitivity of the material to partial corrosion. When the NaCl concentration is increased again, the diameter of the corrosion pit remains unchanged, and the width and depth of typical examples of corrosion pitting are shown in Fig. 11. The accelerating role of NaCl in enhancing the corrosion process decreases if the concentration exceeds a certain value in solution [15], which is in agreement with the EIS results.

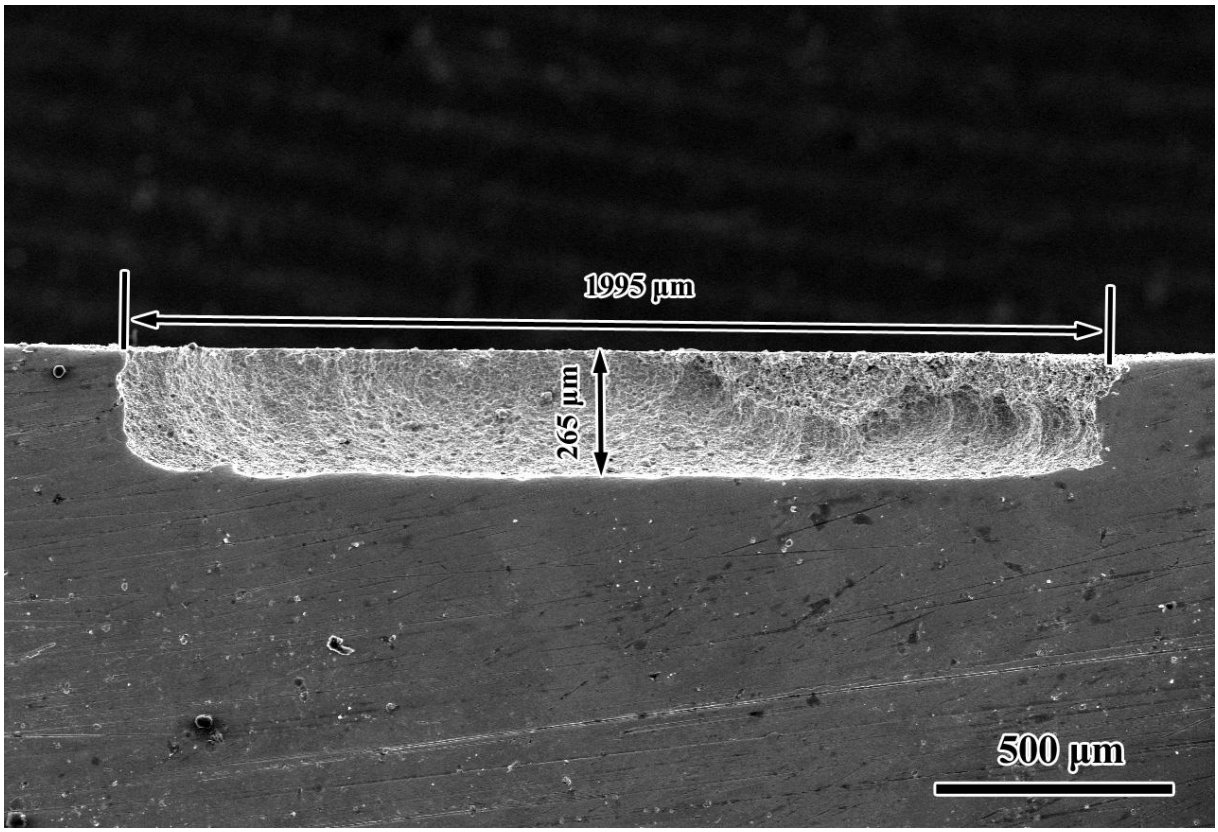

Figure 11. Cross-section of a pit on the steel surface after a 21 day exposure in the 10% NaCl solution

From this discussion, the existence of NaCl can promote uniform corrosion and the formation and development of corrosion pitting. In NaCl solutions with low concentrations, T92 steel undergoes uniform corrosion, whereas its corrosion model will develop into corrosion pitting as the concentration of NaCl is increased.

3.6 Formation and development mechanism of corrosion pitting

In this section, we divide the formation process of corrosion pitting on T92 steel into two stages, namely, nucleation and growth [19], and discuss their mechanisms.

The Cr content of T92 steel is approximately 9%, which is sufficient to form a passivation film during corrosion. In NaCl solutions, there will be a layer of passivation film combined with Fe/Cr oxides that form on the steel surface, which is part of the dynamic balance of "formation-damage" [20]. Due to the small radius, it is easy for chlorine to penetrate through the solution/passive film interface into the passive film via weak spots in the passive film (inclusions, dislocations, alloy phases, etc.) [21]. Thus, the compactness and integrity of the passive film is damaged, greatly decreasing its protective capacity. Then, chlorine will continue to expand access the passive film and arrive at the passive film/metal interface. Afterwards, the chlorine may segregate near one weak spot and induce the core of corrosion pitting. Additionally, during the dynamic balance of "formation-damage", Cl^- can

take part in and accelerate the "damage" process of the passive film, forming the core of corrosion pitting.

After the formation of the core of corrosion pitting, an incubation period is required for small corrosion pits to nucleate and grow steadily on the steel surface. At this moment, Cl^- enriches in internal holes, and the hydrolysis of Fe^{3+}/Fe^{2+} and Cr^{2+} leads to the acidification of the solution in the holes. The repassivation potential of the steel in the holes increases under acidic conditions (i.e., repassivation will be more difficult), and the ion concentration and conductivity increase in the holes. These conditions cause the steel in the holes to be maintained in the activated state. However, the corresponding cathodic reaction may occur on the surrounding surface of the hole, generating a galvanic couple of a large cathode/small anode. This will accelerate the corrosion rate of the T92 steel and finally cause the holes to develop into a pitting morphology, as shown in Figs. 8-10.

4. CONCLUSION

1. The corrosion rate of T92 steel continuously increases with the NaCl concentration during neutral salt spray testing.

2. NaCl promotes the anodic, rather than cathodic, process of T92 steel in solution.

3. In NaCl solutions with low concentrations, T92 steel undergoes uniform corrosion, whereas its corrosion model will develop into corrosion pitting as the concentration of NaCl increases.

4. The formation process for corrosion pitting on T92 steel can be divided into two stages, nucleation and growth. NaCl plays important roles in both the nucleation and growth processes.

ACKNOWLEDGEMENTS

We are very grateful to the anonymous reviews and the editor for the instructive comments, which are invaluable for the quality improvement of the paper. We are grateful for financial support of the National Natural Science Foundation of China (51601164, 51471176 and 51561033) and Opening Foundation of Key Laboratory of Materials Design and Preparation Technology of Hunan Province(KF20140702) and Xiangtan University Fund (15ZXZ15).

References

1. Y. Otoguro, M. Matsubara, I. Itoh, T. Nakazawa, *Nucl. Eng. Des.* 196 (2000)51.
2. C. P. O'Hagana, B. J. O'Brienc, S. B. Leena, R. F.D. Monaghana, *Corros. Sci.* 109(2016)101.
3. J. Liu, Z. Jiang, S. Tian, Q. Huang, Y. Liu, *J. Nucl. Mater.* 468 (2016)299.
4. N. Zhang, H. Xu, B. Li, Y. Bai, D. Liu, *Corros. Sci.* 56(2012)123.
5. X. Ren, K. Sridharan, T. R. Allen, *J. Nucl. Mater.* 358 (2006)227.
6. Y. Chen, K. Sridharan, T. Allen, *Corros. Sci.* 48 (2006) 2843.
7. P. Ampornrat, G. S. Was, *J. Nucl. Mater.* 371 (2007) 1.
8. P. Kofstad, High Temperature Corrosion, Elsevier Applied Science Publishers Ltd., London, 1988.
9. L. Tomlinson, N. J. Cory, *Corros. Sci*. 29(1989)939.
10. D. Zhang, J. Xu, G. Zhao, Y. Guan, M. Li, Chin. *J. Mater. Res.* 22(2008)599.
11. X. Li, X. Gang, J. He, *J. Chin. Soc. Corros. Prot.* 22(2002)101.

12. L. Zhang, Q. Wang, C. Liu, *Baosteel Technol.* 4(2014)6.
13. F. Yu, C. Yuan, Y. Jiang, Y. Lin, *Total Corros. Contr.* 24(4)(2010)6.
14. J.H. Liu, C. Wen, M. Yu, S.M. Li, B. Wang, *Int. J. Electrochem. Sci.*, 8 (2013) 4085.
15. A. Hamdy, E. El-Shenawy, T. El-Bitar, *Int. J. Electrochem. Sci.*, 1 (2006) 171.
16. J. Liu, K. Zhao, M. Yu, S. Li, C. Wen, *Int. J. Electrochem. Sci.*, 9 (2014) 3246.
17. T. Wu, J. Xu, C. Sun, M. Yan, C. Yu, W. Ke, *Corros. Sci.*, 88 (2014) 291.
18. C. Wen, M. Yu, S. Li, X. Li, J. Liu, *Int. J. Electrochem. Sci.*, 9 (2014) 5803.
19. O.A. Hazzazi, A.M. Zaky, *Int. J. Electrochem. Sci.*, 3 (2008) 489.
20. T. P. Hoar, D. C. Mears, G.P. Rothwell, *Corros. Sci.* 5(1965)279.
21. H. H. Strehblow, *Mater. Corros.* 27(1976)792.